Computing and Informatics, Vol. 26, 2007, 17–31

IMAGE SEGMENTATION BY FUZZY C-MEANS CLUSTERING ALGORITHM WITH A NOVEL PENALTY TERM

Yong YANG

School of Information Management
Jiangxi University of Finance and Economics
Nanchang 330013, P. R. China
e-mail: greatyyy765@sohu.com

Shuying HUANG

School of Electronics
Jiangxi University of Finance and Economics
Nanchang 330013, P. R. China

Manuscript received 23 February 2005; revised 9 June 2006
Communicated by Steve J. Maybank

Abstract. To overcome the noise sensitiveness of conventional fuzzy c-means (FCM) clustering algorithm, a novel extended FCM algorithm for image segmentation is presented in this paper. The algorithm is developed by modifying the objective function of the standard FCM algorithm with a penalty term that takes into account the influence of the neighboring pixels on the centre pixels. The penalty term acts as a regularizer in this algorithm, which is inspired from the neighborhood expectation maximization algorithm and is modified in order to satisfy the criterion of the FCM algorithm. The performance of our algorithm is discussed and compared to those of many derivatives of FCM algorithm. Experimental results on segmentation of synthetic and real images demonstrate that the proposed algorithm is effective and robust.

Keywords: Fuzzy c-means; clustering; image segmentation; expectation maximization

1 INTRODUCTION

Image segmentation is an important and challenging problem and a necessary first step in image analysis as well as in high-level image interpretation and understanding such as robot vision, object recognition, and medical imaging. The goal of image segmentation is to partition an image into a set of disjoint regions with uniform and homogeneous attributes such as intensity, colour, tone or texture, etc. Many different segmentation techniques have been developed and detailed surveys can be found in references [1–3]. According to reference [1], the image segmentation approaches can be divided into four categories: thresholding, clustering, edge detection and region extraction. In this paper, a clustering based method for image segmentation will be considered.

Clustering is a process for classifying objects or patterns in such a way that samples of the same group are more similar to one another than samples belonging to different groups. Many clustering strategies have been used, such as the hard clustering scheme and the fuzzy clustering scheme, each of which has its own special characteristics. The conventional hard clustering method restricts each point of the data set to exclusively just one cluster. As a consequence, with this approach the segmentation results are often very crisp, i.e., each pixel of the image belongs to exactly just one class. However, in many real situations, for images, issues such as limited spatial resolution, poor contrast, overlapping intensities, noise and intensity inhomogeneities variation make this hard (crisp) segmentation a difficult task. Thanks to the fuzzy set theory [4] was proposed, which produced the idea of partial membership of belonging described by a membership function; fuzzy clustering as a soft segmentation method has been widely studied and successfully applied in image segmentation [7–14]. Among the fuzzy clustering methods, fuzzy c-means (FCM) algorithm [5] is the most popular method used in image segmentation because it has robust characteristics for ambiguity and can retain much more information than hard segmentation methods [6]. Although the conventional FCM algorithm works well on most noise-free images, it has a serious limitation: it does not incorporate any information about spatial context, which cause it to be sensitive to noise and imaging artifacts.

To compensate for this drawback of FCM, the obvious way is to smooth the image before segmentation. However, the conventional smoothing filters can result in loss of important image details, especially image boundaries or edges. More importantly, there is no way to rigorously control the trade-off between the smoothing and clustering. Other different approaches have been proposed ([8–13]). Tolias et al. [8] proposed a fuzzy rule-based scheme called the rule-based neighborhood enhancement system to impose spatial continuity by post-processing on the clustering results obtained using FCM algorithm. In their another approach [9], spatial constraint is imposed in fuzzy clustering by incorporating the multi-resolution information. Noordam et al. [10] proposed a Geometrically Guided FCM (GG-FCM) algorithm based on a semi-supervised FCM technique for multivariate image segmentation. In their work, the condition of each pixel is determined by the membership values of surrounding neighboring pixels and then is either added to or subtracted from the cluster. Recently, some approaches ([11–13]) were proposed for increasing the robustness of FCM to noise by directly modifying the objective function. In [11], a regularization term was introduced into the standard FCM to impose the neighborhood effect. Later, Zhang et al. [12] incorporated this regularization term into a kernel-based fuzzy clustering algorithm. More recently, Li et al. [13] incorporated this regularization term into the adaptive FCM (AFCM) algorithm [14] to overcome the noise sensitivity of AFCM algorithm. Although the latter two methods are claimed to be more robust to noise, they show considerable computational complexity.

In this paper, a novel extended FCM clustering method, called penalized FCM (PFCM) algorithm is presented for image segmentation. The penalty term takes the spatial dependence of the objects into consideration, which is inspired by the Neighborhood EM (NEM) algorithm [15] and is modified according to the FCM criterion. Minimizing this new objective function according to the zero gradient condition, the PFCM algorithm is then proposed which can handle both the feature space information and spatial information during segmentation. The advantage of this algorithm is that it can handle small and large amounts of noise by adjusting a penalty coefficient. In addition, in this algorithm the membership is changed while the centroid computations are the same as in the standard FCM algorithm. Hence, it is easy to implement. Experimental results and comparisons with many derivatives of FCM algorithm on a variety of images show the proposed algorithm is effective and robust.

The rest of this paper is organized as follows. Section 2 briefly describes the theory of FCM and NEM algorithms. The PFCM algorithm is presented in Section 3. Experimental results and comparisons are given in Section 4. Finally, some conclusions are drawn in Section 5.

2 REVIEW OF RELATED THEORY

2.1 Fuzzy C-Means Clustering Algorithm

The Fuzzy C-Means (FCM) clustering algorithm was first introduced by Dunn [16] and later was extended by Bezdek [5]. The algorithm is an iterative clustering method that produces an optimal c partition by minimizing the weighted within group sum of squared error objective function J_{FCM} [5]:

$$J_{FCM} = \sum_{k=1}^{n} \sum_{i=1}^{c} (u_{ik})^q \, d^2 (x_k, v_i) \tag{1}$$

where $X = \{x_1, x_2, \cdots, x_n\} \subseteq R^p$ is the data set in the p-dimensional vector space, n is the number of data items, c is the number of clusters with $2 \leq c < n$, u_{ik} is the degree of membership of x_k in the i^{th} cluster, q is a weighting exponent on each fuzzy membership, v_i is the prototype of the centre of cluster i, $d^2(x_k, v_i)$ is a distance measure between object x_k and cluster centre v_i. A solution of the object function J_{FCM} can be obtained via an iterative process, which is carried out as follows:

1. Set values for c, q and ϵ.
2. Initialize the fuzzy partition matrix $U = [u_{ik}]$.
3. Set the loop counter $b = 0$.
4. Calculate the c cluster centers $\left\{v_i^{(b)}\right\}$ with $U^{(b)}$:

$$v_i^{(b)} = \frac{\sum\limits_{k=1}^{n} \left(u_{ik}^{(b)}\right)^q x_k}{\sum\limits_{k=1}^{n} \left(u_{ik}^{(b)}\right)^q} \tag{2}$$

5. Calculate the membership $U^{(b+1)}$. For $k = 1$ to n, calculate the following: $I_k = \{i\,|1 \le i \le c, d_{ik} = \|x_k - v_i\| = 0\}$, $\not I$; for the k^{th} column of the matrix, compute new membership values:
   (a) if $I_k = \phi$, then
   $$u_{ik}^{(b+1)} = \frac{1}{\sum_{j=1}^{c} \left(\frac{d_{ik}}{d_{jk}}\right)^{\frac{2}{(q-1)}}}, \tag{3}$$
   (b) else $u_{ik}^{(b+1)} = 0$ for all $i \notin I$ and $\sum_{i \in I_k} u_{ik}^{(b+1)} = 1$; next k.
6. If $\left\|U^{(b)} - U^{(b+1)}\right\| < \epsilon$, stop; otherwise, set $b = b + 1$ and go to step 4.

2.2 Neighborhood EM Algorithm

In order to incorporate the spatial dependence into the objects, a modified version of the conventional expectation maximization (EM) [17] algorithm has been proposed in [15]. In this approach, the maximum likelihood criterion is penalized by a term that quantifies the degree of spatial contiguity of the pixels supporting the respective components of the probability density function (pdf) model. The spatial structure of a given data set is defined by using matrix $W = (w_{jk})$:

$$w_{jk} = \begin{cases} 1 & \text{if } x_j \text{ and } x_k \text{ are neighbors and } j \neq k, \\ 0 & \text{otherwise.} \end{cases} \tag{4}$$

The following term is then used for regularizing the maximum likelihood criterion

$$G(c) = \frac{1}{2} \sum_{j=1}^{n} \sum_{k=1}^{n} \sum_{i=1}^{c} c_{ij} c_{ik} w_{jk}, \tag{5}$$

where c is the number of classes and c_{ij} is the probability that x_j belongs to class i. This term characterizes the homogeneity level of the partition. The more the classes contain adjacent elements, the greater this term is. The new criterion of the NEM algorithm is obtained by optimizing the weighted sum of two terms

$$U(c, \phi) = D(c, \phi) + \beta G(c), \tag{6}$$

where $D(c, \phi)$ is the log-likelihood function of EM algorithm, $\beta > 0$ is a fixed coefficient. Details about NEM can be found in [15]. This algorithm is maximized to get the optimum results just as the same structure as the PersonNameProductIDEM algorithm. SuccessfulEM algorithm. Successful results have been reported for image segmentation using this algorithm.

3 PENALIZED FCM ALGORITHM

It is noted from (1) that the objective function of the traditional FCM algorithm does not take any spatial information into account; this means the clustering process is related only to gray levels independently of pixels of the image in segmentation. This limitation makes FCM very noise-sensitive. The general principle of the technique presented in this paper is to incorporate the neighborhood information into the FCM algorithm during classification. In order to incorporate the spatial context into FCM algorithm, the objective function of (1) is penalized by a regularization term, which is inspired by the above NEM algorithm and modified based on the FCM algorithm criterion. The new objective function of the PFCM is defined as follows

$$J_{PFCM} = \sum_{k=1}^{n} \sum_{i=1}^{c} (u_{ik})^q d^2(x_k, v_i) + \gamma \sum_{k=1}^{n} \sum_{j=1}^{n} \sum_{i=1}^{c} (u_{ik})^q (1 - u_{ij})^q w_{kj}, \tag{7}$$

where w_{kj} is defined as (4). The parameter γ (≥ 0) controls the effect of the penalty term. The relative importance of the regularizing term is inversely proportional to the signal-to-noise (SNR) of the image. placeLower SNR would require a higher value of the parameter γ, and vice versa. When $\gamma = 0$, J_{PFCM} equals to J_{FCM}. The major difference between NEM algorithm and PFCM algorithm is that the penalty term in the NEM is maximized to get the solutions while in the PFCM it should be minimized in order to satisfy the principle of FCM algorithm. Besides, the penalty term in the PFCM algorithm has the weighting exponent q to control the degree of fuzziness in the resulting membership function contrary to the penalty term in the NEM algorithm that is crisp. This new penalty term is minimized when the membership value for a particular class is large and the membership values for the same class at neighboring pixels is also large, and vice versa. In other words, it constrains the pixel's membership value of a class to be correlated with those of the neighboring pixels.

The objective function J_{PFCM} can be minimized in a fashion similar to the standard FCM algorithm. An iterative algorithm for minimizing (7) can be derived by evaluating the centroids and membership functions that satisfy a zero gradient condition. The constrained optimization in (7) will be solved using one Lagrange multiplier:

$$\eta_q = \sum_{k=1}^{n}\sum_{i=1}^{c}(u_{ik})^q\, d^2(x_k, v_i) + \gamma\sum_{k=1}^{n}\sum_{j=1}^{n}\sum_{i=1}^{c}(u_{ik})^q(1-u_{ij})^q w_{kj} + \lambda\left(1-\sum_{i=1}^{c}u_{ik}\right). \tag{8}$$

Taking the partial derivate of (8) with respect to u_{ik} and setting the result to zero yields

$$\left[\frac{\partial \eta_q}{\partial u_{ik}} = q(u_{ik})^{q-1} d^2(x_k, v_i) + \gamma q(u_{ik})^{q-1}\sum_{j=1}^{n}(1-u_{ij})^q w_{kj} - \lambda\right]_{u_{ik}=u_{ik}^*} = 0. \tag{9}$$

Solving for u_{ik}^*, we have

$$u_{ik}^* = \left(\frac{q\left(d^2(x_k, v_i) + \gamma\sum_{j=1}^{n}(1-u_{ij})^q w_{kj}\right)}{\lambda}\right)^{\frac{-1}{(q-1)}}. \tag{10}$$

Since $\sum_{l=1}^{c} u_{lk} = 1$, $\forall k$, this constraint equation is then employed, yielding

$$\sum_{l=1}^{c}\left(\frac{q\left(d^2(x_k, v_l) + \gamma\sum_{j=1}^{n}(1-u_{lj})^q w_{kj}\right)}{\lambda}\right)^{\frac{-1}{(q-1)}} = 1. \tag{11}$$

Solving λ from (11), we have

$$\lambda = \frac{q}{\left(\sum_{l=1}^{c}\left(\frac{1}{d^2(x_k,v_l)+\gamma\sum_{j=1}^{n}\left(1-u_{lj}\right)^q w_{kj}}\right)^{\frac{1}{(q-1)}}\right)^{q-1}}. \tag{12}$$

Combining (12) and (10), the zero-gradient condition for the membership estimator can be written as

$$u_{ik}^* = \frac{1}{\sum_{l=1}^{c}\left(\frac{d^2(x_k,v_i)+\gamma\sum_{j=1}^{n}(1-u_{ij})^q w_{kj}}{d^2(x_k,v_l)+\gamma\sum_{j=1}^{n}\left(1-u_{lj}\right)^q w_{kj}}\right)^{\frac{1}{q-1}}}. \tag{13}$$

Similarly, taking the equation (8) with respect to v_i and setting the result to zero, we have

$$v_i^* = \frac{\sum_{k=1}^{n}(u_{ik})^q x_k}{\sum_{k=1}^{n}(u_{ik})^q}. \tag{14}$$

which is identical to that of FCM because in fact the penalty function in (7) does not depend upon v_i. Thus, the PFCM algorithm is given as follows:

PFCM algorithm

Step 1: Set the cluster centroids v_i, fuzzification parameter q, the values of c and ϵ.

Step 2: Calculate membership values using (13).

Step 3: Compute the cluster centroids using (14).

Step 4: Go to step 2 and repeat until convergence.

When the algorithm has converged, a defuzzification process takes place then in order to convert the fuzzy partition matrix U to a crisp partition. A number of methods have been developed to defuzzify the partition matrix U, among which the maximum membership procedure is the most important. The procedure assigns object k to the class C with the highest membership:

$$C_k = \arg_i \{\max(u_{ik})\}, i = 1, 2, \ldots, c. \quad (15)$$

With this procedure, the fuzzy images are then converted to crisp image that is segmentation.

4 EXPERIMENTAL RESULTS

In this section, the application results of the PFCM algorithm are presented. The performance of the proposed method is compared with those of standard FCM algorithm [5], spatial FCM (SFCM) algorithm [11], and kernel-based fuzzy clustering with spatial constraints (SKFC) technique [12]. For all cases, unless otherwise stated, the weighting exponent $q = 2.0$, $\epsilon = 0.0001$ and $\gamma = 400$, where the parameter γ is selected experimentally in order to give appropriate results. If the image is more noisy, a larger parameter γ is needed. A 3×3 window of image pixels is considered in this paper, thus the spatial influence on the centre pixel is through its 8-neighborhood pixels. For the sake of simplicity, in all the examples, the parameter α in SFCM is set to be 0.8 and the parameters in SKFC are set as follows: $\alpha = 3$, $\sigma = 150$. All the algorithms are coded in Microsoft Visual C++ Version 6.0 and are run on a 1.7 GHz Pentium IV personal computer with a memory of 256 MB.

To evaluate the performance of the proposed approach, tests were first realized on two synthetic images. First, we generate a simple two-class synthetic image, whose intensity values are 100 and 60, respectively, and the image size is 256×256. The image is then corrupted by 5 % Gaussian noise, which is shown in Figure 1 a). Figure 1 e) shows the result of the PFCM algorithm. The results for comparison of FCM, SFCM and SKFC are given in Figure 1 b), c) and d), respectively. As can be seen, without spatial information constraints FCM algorithm can not even separate the two classes. Although the SFCM algorithm can segment the image into two parts, many noises still exist in both regions. Our PFCM approach can get comparable result as SKFC algorithm and outperforms the conventional FCM and SFCM algorithms in the noisy situation. The number of misclassified pixels and the consuming time for different methods are counted during the experiments and listed in Table 1. It can be seen from Table 1 that the total number of the misclassification pixels for the PFCM algorithm is the least in the four methods, and the misclassified number for FCM algorithm is about 452 times that of the proposed method. Also, it is important to be noted from Table 1 that the consuming time for SKFC is the longest in the four algorithms, and PFCM and SFCM algorithms cost almost the same time after convergence.

Segmentation method	FCM	SFCM	SKFC	PFCM
Misclassified number	4 520	386	17	10
Consuming time	1 s	2 s	12 s	2 s

Table 1. Number of misclassified pixels and consuming time with different methods for Figure 1 a)

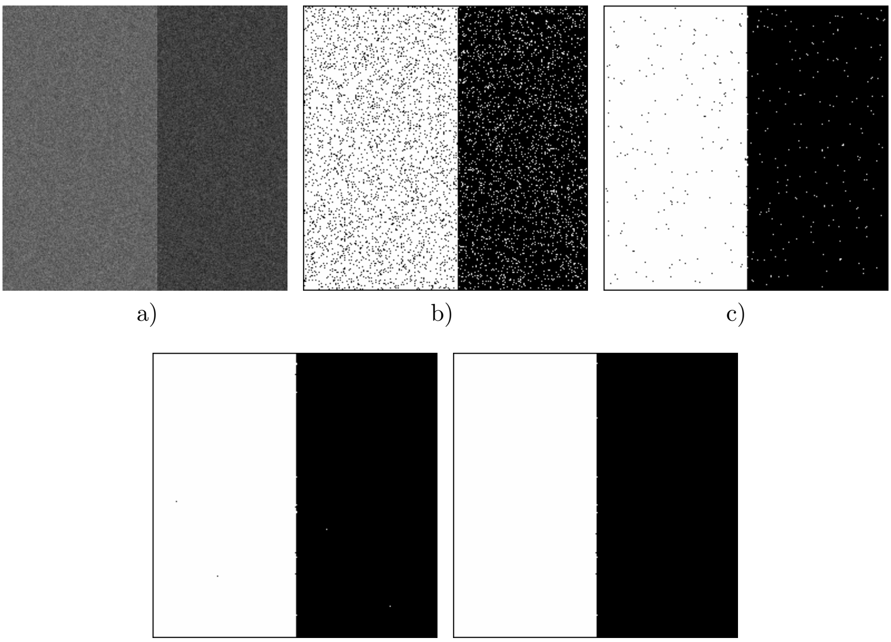

a) b) c) d) e)

Fig. 1. Comparison of segmentation results on a two-class synthetic image corrupted by 5 % Gaussian noise: a) The original image, b) FCM result, c) SFCM result, d) SKFC result, e) PFCM result

Second, a multiple-class synthetic image has been created, in which the intensity values are 0, 255, and 128 respectively, and the image size is 256 × 256. Additive 10 % Gaussian noise was then added to the image. To get a better insight, the image is segmented by the four algorithms into three corresponding classes with intensity values 255, 0, and 128 representing class 1, class 2 and class 3, respectively. Figure 2 a) shows the test degraded noisy images. The results of FCM, SFCM, SKFC and PFCM algorithms are shown in Figures 2 b), c), d) and e), respectively. We observed that the three regions are well brought out by these four algorithms. However, with the FCM algorithm, the segmentation result still has many noises, especially in class 1 and class 3, while the result obtained by PFCM algorithm is less speckled and smoother; this is almost identical to those of the SFCM and SKFC algorithms. Again, the number of misclassified pixels and the consuming time for different methods are counted during the experiments and listed in Table 2. It can be seen from Table 2 that the total number of misclassification pixels for the FCM algorithm is nearly 63 times that of the proposed method. Both these two synthetic examples can demonstrate that the incorporation of the spatial neighborhood constraints into the FCM algorithm can significantly improve the segmented result when noise is present. Although the SKFC algorithm can get nearly the same results as the proposed PFCM algorithm, it consumes more computational time.

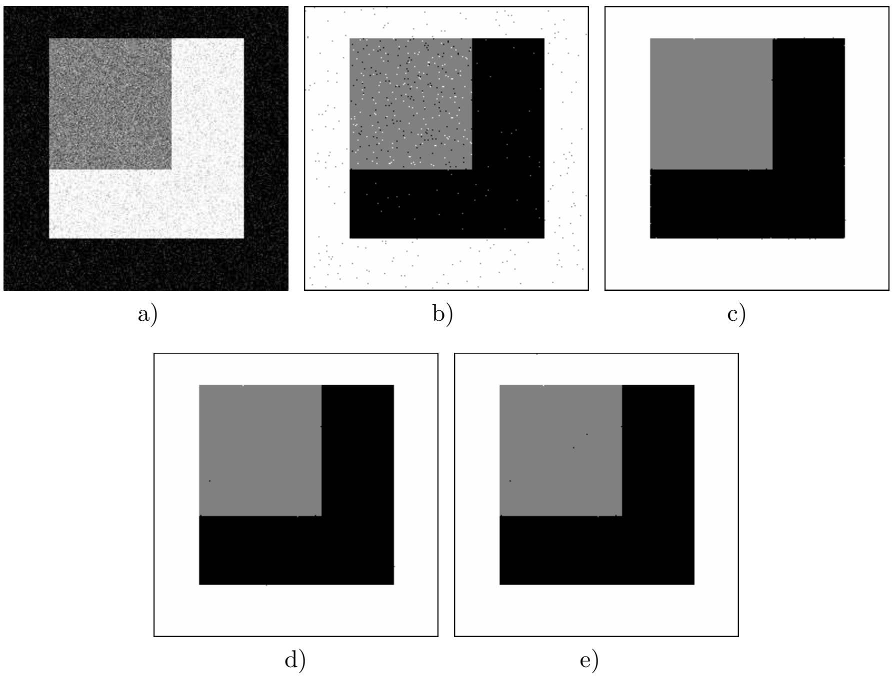

Fig. 2. Comparison of segmentation results on a three-class synthetic image corrupted by 10 % Gaussian noise: a) The original image, b) FCM result, c) SFCM result, d) SKFC result, e) PFCM result

We take a set of values for γ to test its effect on the performance of PFCM algorithm. Figure 3 shows the classifications errors under different values of γ on a synthetic image corrupted by Gaussian noise. It is noted from Figure 3 that, as

Segmentation method	FCM	SFCM	SKFC	PFCM
Class 1	185	9	2	1
Class 2	42	14	1	1
Class 3	337	4	5	7
Total	564	27	8	9
Consuming time	2 s	4 s	30 s	2 s

Table 2. Number of misclassified pixels and consuming time with different methods for Figure 2 a)

γ increases, the number of misclassified pixels of the algorithm reduces and there are no apparent changes after $\gamma = 400$. In fact, these algorithms can reach minima and the performance is stable between $\gamma = 400$ and $\gamma = 500$.

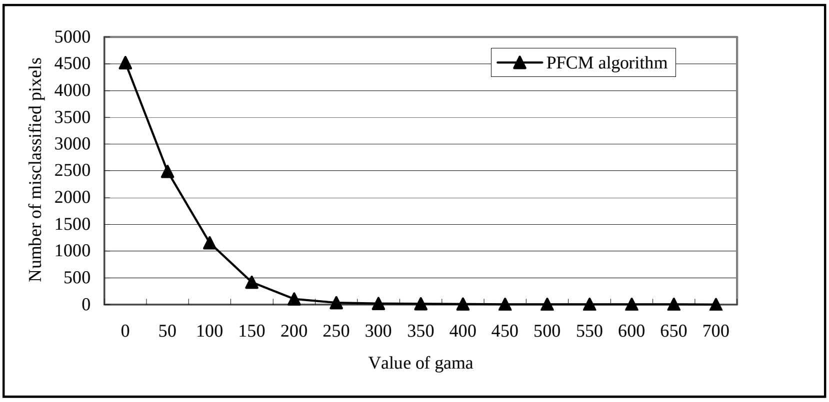

Fig. 3. Comparison of classification errors under different value of γ of PFCM algorithm

The second type example is a simulated magnetic resonance (MR) brain image obtained from the BrainWeb Simulated Brain Database [18]. This brain image was simulated with T1-weighted contrast, 1-mm cubic voxels, 7% noise and no intensity inhomogeneity. Before segmentation, the non-brain parts of the image such as the bone, cortex and fat tissues have been removed firstly. The class number of the image was assumed to be four, corresponding to gray matter (GM), white matter (WM), cerebrospinal fluid (CSF) and background (BKG). The parameter γ is set to be metricconverterProductID500 in500 in this experiment. Figure 4 a) shows a slice from the simulated data set, Figures 4 b)–e) show the segmentation results obtained by applying FCM, SFCM, SKFC and PFCM algorithms, respectively; the ground truth is given in Figure 4 f). It is clearly seen that the proposed method performs the best in the four algorithms and its result is much closer to the ground truth. The result of PFCM is more homogeneous and smoother than other three algorithms especially in the region of WM, which again indicates our method is effective and robust to noise. To measure the segmentation accuracy, we also apply the quantitative evaluation of performance by using the overlap metric criteria [19]. The overlap metric is a measure for comparing two segmentations that is defined for a given class assignment as the sum of the number of pixels that both have the class assignment in each segmentation divided by the sum of pixels where either segmentation has the class assignment. "Larger metric" means "more similar for results". The overlap metrics of WM, GM, CSF and BKG are given in Table 3. As can be seen from Table 3, with spatial constraints, SFCM, SKFC and PFCM algorithms can achieve much better performance than standard FCM algorithm. However, utilized by the PFCM algorithm, the overlap metrics of WM and GM have been increased more greatly compared to other three algorithms. In this example, the consuming time for FCM is 2 s, for SFCM and PFCM is 7 s, while for SKFC it is 45 s.

To test the performance of the four algorithms under other level of noises on the Simulated Brain Database [18], we do the following comparison experiments. Figure 5 shows the segmentation accuracy of applying these algorithms to the images with different level of noises. The segmentation accuracy (SA) is defined as follows:

$$SA = \frac{\text{Number of correctly classified pixels}}{\text{Total number of pixels}} \times 100. \tag{16}$$

Obviously, with noise level increase the segmentation result of FCM degrades rapidly, while the fuzzy clustering algorithms with spatial constraints such as SFCM, SKFC and PFCM can overcome the problem caused by noise. Generally, the PFCM and SKFC algorithms produce comparable results, which are a little better than those of the SFCM algorithm. However, it should be noted that the SKFC algorithm usually consumes much more computational time than PFCM algorithm.

Segmentation method	WM	GM	CSF	BKG
FCM	0.896	0.868	0.876	0.989
SFCM	0.942	0.897	0.916	0.990
SKFC	0.938	0.900	0.912	0.991
PFCM	0.977	0.931	0.894	0.991

Table 3. Overlap metrics with different methods for Figure 4 a)

In the last examples, there are two groups of real standard test images named *placeLena* and *Cameraman* without adding any type of noise. In both experiments, the class number c is set to 2. The original images are shown in Figure 6 a), where the top is *placeLena* and the bottom is *Cameraman*. Due to the results of SFCM, SKFC are almost similar to that of the PFCM algorithm; they are not given here again. The results of the FCM and PFCM algorithms are presented in Figures 6 b) and c), respectively. As can be seen, both FCM and PFCM algorithms can well extract the object from the background in each image. However, it is important to note the proposed method performs better for the segmentation with more homogeneous regions such as the face, the shoulder and the cap of *placeLena*, and with least

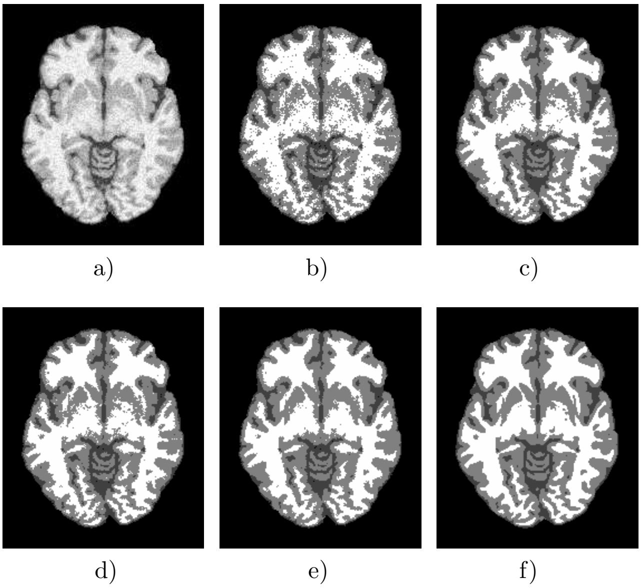

Fig. 4. Comparison of segmentation results on a MR phantom corrupted by 7 % Gaussian noise and no intensity inhomogeneity: a) The original images, b) FCM results, c) SFCM result, d) SKFC result, e) PFCM results, f) Ground truth

spurious components and noises particularly in the grass ground area of *Cameraman*. The results presented here can prove that our method is capable of coping with not only noises but also artifacts in the image.

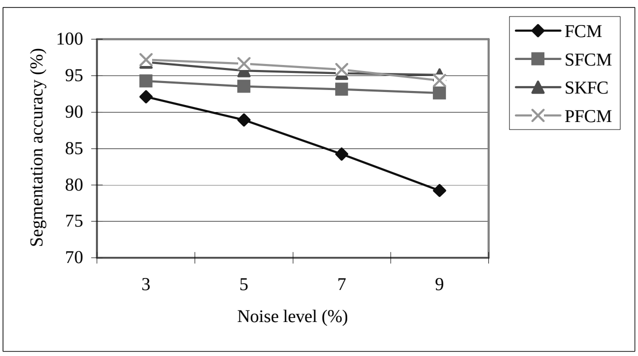

Fig. 5. Comparison of segmentation accuracy of different methods on simulated brain MR images under different level of noises

a) b) c)

Fig. 6. Comparison of segmentation results on real standard images named *placeLena* and *cameraman*, a) The original images, b) FCM results, c) PFCM results

5 CONCLUSIONS

We have presented a novel extended FCM algorithm, PFCM algorithm that is able to incorporate both local spatial contextual information and feature space information into the image segmentation. The algorithm is formulated by incorporating the spatial neighborhood information into the original FCM algorithm with a penalty term, which is inspired by the NEM algorithm and is modified in order to satisfy the criterion of the FCM algorithm. A variety of images, including synthetic, simulated and real images were used to compare the performance of FCM, SFCM, SKFC and PFCM algorithms. Experimental results show that the proposed method is effective and more robust to Gaussian noise and other artifacts than the conventional FCM algorithm in image segmentation. Future work will focus on adaptively deciding the penalized parameter of this algorithm as well as compensating for the intensity inhomogeneity while segmenting the image data.

Acknowledgments

This work is supported by the Science and Technology Research Project of the Education Department of Jiangxi Province (No. 2007-270), and the author would like to thank the anonymous referees for their valuable suggestions.

REFERENCES

[1] Fu, S. K.—Mui, J. K.: A Survey on Image Segmentation. Pattern Recognition, Vol. 13, 1981, pp. 3–16.

[2] Haralick, R. M.—Shapiro, L. G.: Image Segmentation Techniques. Comput. Vision Graphics Image Process., Vol. 29, 1985, pp. 100–132.

[3] Pal, N.—Pal, S.: A Review on Image Segmentation Techniques. Pattern Recognition, Vol. 26, 1993, pp. 1277–1294.

[4] Zadeh, L. A.: Fuzzy Sets. Inform. and Control., Vol. 8, 1965, pp. 338–353.

[5] Bezdek, J. C.: Pattern Recognition with Fuzzy Objective Function Algorithms. New York: Plenum Press, 1981.

[6] Bezdek, J. C.—Hall, L. O.—Clarke, L. P.: Review of MR Image Segmentation Techniques Using Pattern Recognition. Med. Phys., Vol. 20, 1993, pp. 1033–1048.

[7] Kwon, M. J.—Han, Y. J.—Shin, I. H.—Park, H. W: Hierarchical Fuzzy Segmentation of Brain MR Images. International Journal of Imaging Systems and Technology, Vol. 13, 2003, pp. 115–125.

[8] Tolias, Y. A.—Panas, S. M.: On Applying Spatial Constraints in Fuzzy Image Clustering Using a Fuzzy Rule-Based System. IEEE Signal Processing Letters, Vol. 5, 1998, pp. 245–247.

[9] Tolias, Y. A.—Panas, S. M.: Image Segmentation by a Fuzzy Clustering Algorithm Using Adaptive Spatially Constrained Membership Functions. IEEE Trans. Systems, Man, Cybernet., Vol. 28, 1998, pp. 359–369.

[10] Noordam, J. C.—van den Broek, W. H. A. M—Buydens, L. M. C.: Geometrically Guided Fuzzy C-Means Clustering for Multivariate Image Segmentation. Proc. International Conference on Pattern Recognition, Vol. 1, 2000, pp. 462–465.

[11] Ahmed, M. N.—Yamany, S. M.—Mohamed, N.—Farag, A. A.—Moriarty, T.: A Modified Fuzzy C-Means Algorithm for Bias Field Estimation and Segmentation of MRI Data. IEEE Trans. on Medical Imaging, Vol. 21, 2002, pp. 193–199.

[12] Zhang, D. Q.—Chen, S. C.—Pan, Z. S.—Tan, K. R.: Kernel-Based Fuzzy Clustering Incorporating Spatial Constraints for Image Segmentation. Proc. International Conference on Machine Learning and Cybernetics, Vol. 4, 2003, pp. 2189–2192.

[13] Li, X.—Li, L.—Lu, H.—Chen, D.—Liang, Z.: Inhomogeneity Correction for Magnetic Resonance Images with Fuzzy C-Mean Algorithm. Proc. SPIE Int. Soc. Opt. Eng., Vol. 5032, 2003, pp. 995–1005.

[14] Pham, D. L.—Prince, J. L.: Adaptive Fuzzy Segmentation of Magnetic Resonance Images. IEEE Trans. Medical Imaging, Vol. 18, 1999, pp. 737–752.

[15] Ambroise, C.—Govaert, G.: Convergence of an EM-Type Algorithm for Spatial Clustering. Pattern Recognition Letters, Vol. 19, 1998, pp. 919–927.

[16] Dunn, J. C.: A Fuzzy Relative of the ISODATA Process and its Use in Detecting Compact Well Separated Clusters. Journal of Cybernetics, Vol. 3, 1974, pp. 32–57.

[17] Dempster, A. P.—Laird, N. M.—Rubin, D. B.: Maximum-Likelihood from Incomplete Data Via the EM Algorithm. J. Roy. Statist. Soc., Vol. B39, 1077, pp. 1–38.

[18] Collins, D. L.—Zijdenbos, A. P.—Kollokian, V.—Sled, J. G.—Kabani, N. J. et al.: Design and Construction of a Realistic Digital Brain Phantom. IEEE Trans. MedImaging, Vol. 17, 1998, pp. 463–468.

[19] Available: http://www.bic.mni.mcgill.ca/brainweb/.

Yong Yang received his Ph. D. degree in biomedical engineering from Xi'an Jiaotong University, China in 2005. Now he works in the School of Information Management of Jiangxi University of Finance and Economics. His main areas of interest include pattern recognition, image processing and medical image processing and analysis. He has published nearly 30 scientific papers chiefly in the areas of fuzzy set theoretic and statistical approaches.

Shuying Huang received her Master degree in signal and information engineering from Xi'an University of Technology, China in 2005. Now she works in the School of Electronics of Jiangxi University of Finance and Economics. Her main areas of interest include signal and image processing.